Analyst

ROYAL SOCIETY OF CHEMISTRY

PAPER

View Article Online
View Journal | View Issue



Cite this: *Analyst*, 2021, **146**, 5143

# Long-term migratory velocity measurements of single glioma cells using microfluidics

Esra Sengul[a] and Meltem Elitas *[a,b]

Microfluidic platforms enabling single-cell measurements notably contribute to the identification and observation of rare cancer cells that are involved in tumor invasion. Most aggressive, invasive, and heterogeneous glioblastoma cells cause incurable primary brain tumors. Infiltrating gliomas of a brain tumor microenvironment have been intensively studied using conventional assays. Still, quantitative, simple, and precise tools are required for long-term, steady-state migratory-velocity measurements of single glioma cells. To measure long-term velocity changes and investigate the heterogeneity of glioma cells under different growth conditions, we developed a microfluidic platform. We cultured U87 glioma cells in the microfluidic device using either regular growth medium or conditional medium composed of 50% basal medium and 50% macrophage-depleted medium. We microscopically monitored the behavior of 40 glioma cells for 5 days. Using acquired images, we calculated cellular circularity and determined the migratory velocities of glioma cells from 60 h to 120 h. The mean migratory velocity values of the glioma cells were 1.513 μm $h^{-1}$ in the basal medium and 3.246 μm $h^{-1}$ in the conditional medium. The circularity values of the glioma cells decreased from 0.20–0.25 to 0.15–0.20 when cultured in the conditional medium. Here, we clearly showed that the glioma cells lost their circularity and increased their steady-state velocities; in other words, they adopted an invasive glioma phenotype in the presence of macrophage-depleted medium. Besides, the heterogeneity of the circularity and the velocity of glioma cells were enhanced in the conditional medium.

Received 7th May 2021,
Accepted 29th June 2021

DOI: 10.1039/d1an00817j

rsc.li/analyst



## Introduction

Glioblastoma multiforme (GBM) is the most common and malignant primary brain tumor with a highly complex and heterogeneous tumor microenvironment, resulting in a median survival of about 15 months.[1–3] Its inter- and intra-tumor heterogeneity and invasive characteristics challenge rapid and reliable diagnosis and limit the design of effective treatment strategies.[2] Understanding the invasion and migration of glioma cells might provide new paths for the development of therapeutic strategies and complete resection of gliomas in clinics.[4]

Several publications have reported the genes, proteins and signaling pathways involved in glioma migration and invasion using bulk, conventional methods including tissue microarray, immunohistochemistry, wound migration assay, Boyden chamber/transwell invasion assay, western blot analysis, gene expression profiling, and cell cycle kinetic characterization.[1–8] Using these traditional methods, significant progress has been achieved in the understanding of glioma pathobiology.[9,10]

Recent investigations have focused on the invasiveness of GBM by revealing the dynamic behavior of cells and tumor microenvironments using high-resolution imaging systems, microfluidic platforms, and single-cell analysis tools.[11]

These breakthrough studies used high-resolution, time-lapse imaging to spatiotemporally analyze tumor cell dynamics, using brains of mice, slice cultures generated from a brain or simply Petri dishes.[11–15] For example, Alieva and her group used glioma cells from GBM patients and transplanted these cells into the brain of a mouse. They showed that the border of a tumor had an invasive margin with a slow but direct movement of glioma cells and a diffusive infiltration margin with fast but less directed cellular motion. They quantified the velocity of glioma cells as 2 μm $min^{-1}$ inside the tumor core and 3–5 μm $min^{-1}$ at the margins of the tumor.[11] Demuth's leading-edge work presented the migratory velocity and path of patient-derived cells and TP378MG, TP483MG, G-44, G-168, and G-270 cell lines using acquired time-lapse images of the cells in Petri dishes.[12] They reported that the migratory velocity of the cell lines was in the range of 0–24.2 μm $h^{-1}$ with a mean value of 11.7 μm $h^{-1}$. Chicoine *et al.* performed both *in vitro* and *in vivo* assays to characterize

[a]*Faculty of Engineering and Natural Sciences, Sabanci University, Istanbul 34956, Turkey. E-mail: melitas@sabanciuniv.edu*
[b]*Sabanci University Nanotechnology Research and Application Center, Istanbul 34956, Turkey*

C6 brain tumor cell motility. They reported the velocities of the glioma cells as 1–3 cm $h^{-1}$ and 12.5 μm $h^{-1}$ for *in vitro* and *in vivo* conditions, respectively.[13] When C6 glioma cells were transplanted into the rats and time-lapse microscopy was used to observe glioma migration and proliferation in the brain, the results revealed an unsynchronized, saltatory migration pattern of the glioma cells with an average speed of 25 μm $h^{-1}$.[14]

On the other hand, cutting-edge microchip experiments mostly used micro-patterning techniques and seeded cells on fibronectin-coated polymeric extracellular matrix (ECM) substances to quantify glioma cell migration. When Kiss and his group used this approach without introducing any geometric constraints, the speed of movement was around 23 μm $h^{-1}$ for the U87 glioma cells.[15] Ulrich *et al.* presented the role of ECM rigidity in regulating the tumor cell structure, migration, and proliferation by culturing U373, U87, C6, U251, and SNB19 cell lines on a fibronectin-coated polymeric ECM substance. U87 cells exhibited a 35–40 μm $h^{-1}$ average cell speed on a glass surface.[16] When a 3D collagen gel matrix was used to observe the migration of the patient-derived GBM cell invasion, the average velocity of the observed cell population was 0.12–0.39 μm $min^{-1}$.[17] Monzo *et al.* measured the velocities of the C6 and patient-derived glioma cells using laminin-coated, micropatterned linear tracts by mimicking blood vessels for 18 hours and recorded the average speed of the cells as 52 μm $h^{-1}$.[18] Along this line, Prahl *et al.* reported that U251 cells migrated at a speed of 30 μm $h^{-1}$ in 12 μm × 5 μm enclosed channels.[19] When the chemotaxis-mediated migration speed of glioblastoma cells was monitored across the microchannels, the migration speed of the glioblastoma cells was 10 μm $h^{-1}$.[20]

All these studies verified that glioma cells were highly heterogeneous with random migration patterns and velocities when observed in different microenvironments for several hours. These investigations underline the importance of adequate tools which will allow us to monitor the behavior of glioma cells over a longer period since the cells that were characterized as randomly migrating may show directional migration or uniform velocities after a certain time. To achieve this goal, we determined the migratory velocities and circularities of U87 glioma cells when they were cultured under different growth conditions for 5 days using a microfluidic device.

# Methods

### Batch culture

The U87 (HTB-14™) human glioma and U937 (CRL-1593.2™) human histiocytic lymphoma monocyte cell lines were purchased from ATCC (American Type Culture Collection). The cells were grown in 75 $cm^2$ cell culture flasks and 6-well plates (TTP, Switzerland) at 37 °C with 5% $CO_2$ (NUVE, Turkey). The U87 cells were cultured in DMEM (Dulbecco's modified Eagle's medium), 10% fetal bovine serum (FBS/Sigma-Aldrich, St. Louis, MO), and 1% penicillin/streptomycin (Pen/Strep, Pan Biotech, Germany). The U937 monocytes were maintained in RPMI 1640 medium (Roswell Park Memorial Institute, Pan Biotech, Germany) and 10% FBS (Sigma-Aldrich, St. Louis, MO). The human histiocytic lymphoma macrophages were differentiated from the U937 monocytes, with a density of 3 × $10^5$ cells per ml, in 5 ml of RPMI 1640 and 10% FBS through stimulation of 10 ng $ml^{-1}$ PMA (Phorbol 12-myristate 13-acetate) (PMA, Pan Biotech, Germany).

Macrophage-depleted medium was harvested from U937-differentiated macrophages grown in RPMI 1640 and 10% FBS for 72 h at 37 °C with 5% $CO_2$. The collected medium was centrifuged at 3000 rpm for 5 min using an Eba 20 serial centrifuge (Hettich, Germany) and filtered through a 0.2-μm filter (GVS Filter Technology, United Kingdom). The harvested medium was mixed with DMEM (1 : 1) to obtain the conditional medium. Sengul and Elitas's work[2] showed that 50% basal medium and 50% macrophage-depleted medium did not significantly alter the proliferation rate of U87 glioma cells while introducing macrophage-secreted molecules.[21]

### Microfluidic chip

Fig. 1 shows the PDMS microfluidic platform. We designed the chip using the CleWin 4.0 software and used soft lithography techniques for its fabrication, as explained in detail in Sengul and Elitas's work.[21]

Prior to the experiments, all reagents and microchips were placed in an incubator (37 °C and 5% $CO_2$, NUVE, Turkey) for 30 min to eliminate air bubbles inside the microchannel. Next, a pre-warmed medium was injected into the device before introducing the cells using a 200 μl micropipette (Corning, New York, NY, USA). U87 glioma cells were grown as explained above (see the section Batch culture). Afterwards, we trypsinized (Pan Biotech, Germany) and resuspended the cells in regular growth medium to obtain a cell concentration of 1.6 × $10^5$ cells per ml. Next, 2400 glioma cells in 40 μl were loaded into the microfluidic device. Then, the chips were placed into the incubator (37 °C and 5% $CO_2$, NUVE, Turkey) and their medium was replaced with 40 μl of fresh medium every 24 h. When U87 glioma cells were cultured in conditional settings, their medium was replenished every 24 h with the conditional medium consisting of 50% DMEM and 50% macrophage-depleted medium. There was no significant growth difference for the glioma cells within the regular and conditional culture settings for 120 h.[21] Each experiment was independently performed in duplicate. Fig. 2 illustrates the single-cell analysis performed in the microchip using microscopy images.

### Single-cell migration assay

We performed single-cell migration assays in the microfluidic device for 60 h–120 h, as illustrated in Fig. 1 and 2. Cells were observed using a microscope, and images of the cells were obtained using a Zeiss Axio Observer Z1 inverted microscope equipped with a 10× lens and an AxioCam Mrc5 camera. We manually tracked the positions of the same single cells from 60 h to 120 h using the ImageJ software (Version 2.0). We measured the X/Y coordinates of the single cells according to

 

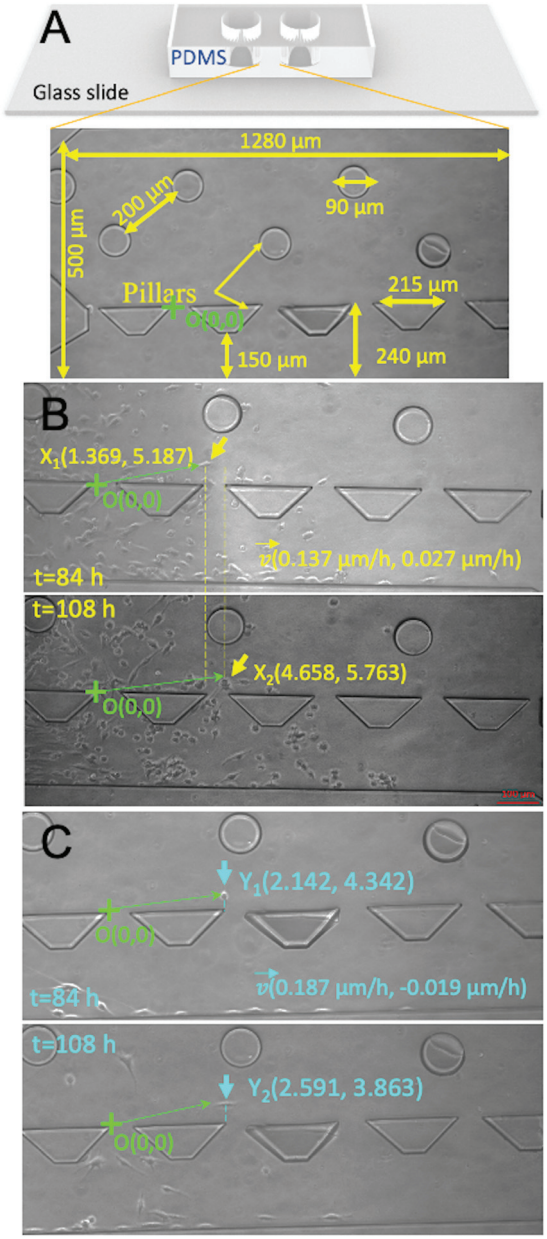


**Fig. 1** Microfluidic cell culture platform. (A) Schematic of the microfluidic channel illustrating the diameters and positions of the circular and trapezoid pillars.[21] U87 glioma cells cultured in (B) regular and (C) conditional media in the microchannels. Positions of the cells are marked by arrows. Origin (O (0, 0), green). Movement of the cell at 84 h and 108 h (scale bar = 100 μm).

the defined origin, as shown in Fig. 1. Next, the obtained data were transferred to Microsoft Excel to calculate migratory velocities of the cells along the $x$ and $y$ axes. Velocities were defined as the ratio of the distance that the cells travelled ($x_2$ and $x_1$ along the $x$-axis, $y_1$ and $y_2$ along the $y$-axis) to the length of the imaging interval ($t_2 - t_1$ = 12 h) as given in eqn(1) and (2), where $v_x$ (μm $h^{-1}$) and $v_y$ (μm $h^{-1}$) are velocities of the cells along the $x$ and $y$ axes, respectively. We visualized and analyzed the cellular circularity using eqn (3), where $A$ is the area

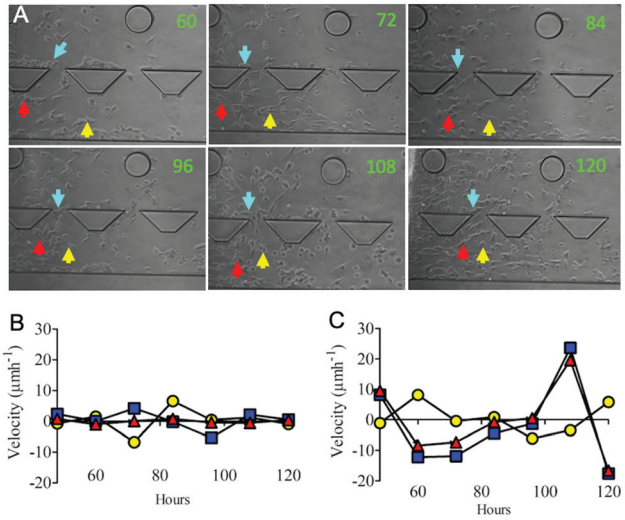


**Fig. 2** Single-cell migration and velocity measurements. (A) U87 glioma cells cultured in regular growth medium for 60–120 h. Positions of the three cells were marked in blue, red, and yellow in the microchannel. Velocities of the cells on the $x$-axis (B) and $y$-axis (C) between 48 h and 120 h. (Pillar diameter = 90 μm.)

(μ$m^2$) and $p$ is the periphery (μm). We visualized and analyzed data using Prism 5 (GraphPad).

$$v_x = \frac{x_2 - x_1}{t_2 - t_1} \quad (1)$$

$$v_y = \frac{y_2 - y_1}{t_2 - t_1} \quad (2)$$

$$\text{Circularity} = \frac{4\pi A}{2p^2} \quad (3)$$

We excluded the first 60 h analysis of cells in the microfluidic channel since the cells were adhered to the glass surface during this period.

### Statistical analysis

We used GraphPad Prism 5.0 for graphical presentation and statistical analysis. The statistical analysis of differences between regular and conditional growth groups of glioma cells was performed using two-way ANOVA for the migratory velocity and unpaired $t$-tests for the quantification of circularities. The histograms of the migratory velocities along the $x$ and $y$ axes of the two groups were presented. The results were considered significant for *: $p < 0.05$, **: $p < 0.01$, and ***: $p < 0.001$. Experiments were performed in independent duplicate, $n = 40$ cells per group. Data are presented as mean ± standard error of the mean (SEM).

## Results

Glioma cells are highly heterogenous with random migration patterns and velocities in different microenvironments, according to observations performed for several hours.[11–20] We per-

formed our microfluidic experiment to monitor the behavior of glioma cells over a longer period to describe whether randomly migrating glioma cells might exhibit directional migration or uniform velocities after a certain time. Fig. 1A shows the microfluidic platform[21] that enables defining the positions of the glioma cells, following their trajectories, and identifying their morphological changes every 12 h from 60 h to 120 h using acquired time-lapse images (see the section Single-cell migration assay). Fig. 1 and 2 illustrate the analysis of individual cell tracks and calculation of the instantaneous migration speed of the cells both in regular (Fig. 1B) and conditional (Fig. 1C) culturing environments. The instantaneous migration speed was calculated as the ratio of the traveled distance of the cell to the length of the imaging interval (eqn (1) and (2), Fig. 2).

Another aspect of our observation was the examination of the influence of geometrically different constraints (trapezoid and circular posts) on cell migration. The presence of the pillars inside the microchannel might influence the migration speed or linearity of the cell trajectories; however, we did not notice geometry-dependent alterations in the migration speeds of the glioma cells.

Fig. 3 illustrates the velocity profiles of single glioma cells from 60 to 120 h in the microfluidic channel. Each color represents a single cell. Velocity changes were separately observed for $x$ and $y$ axes. When the glioma cells were cultured in the regular growth medium, their velocities along the $x$ axes and $y$ axes are presented in Fig. 3A and B, respectively. Fig. 3C and D demonstrate the influence of conditional medium (50% macrophage-depleted medium and 50% regular growth medium) on the migration of the glioma cells through the $x$ and $y$ axes, respectively. Fig. 3B and D show a sudden increase of velocities at 108 h along the $y$ axes when glioma cells were cultured in the regular growth medium.

Fig. 4 displays the comparison of velocity profiles for regular and conditional cultures of glioma cells in the microfluidic device from 60 h to 120 h. Fig. 4A illustrates

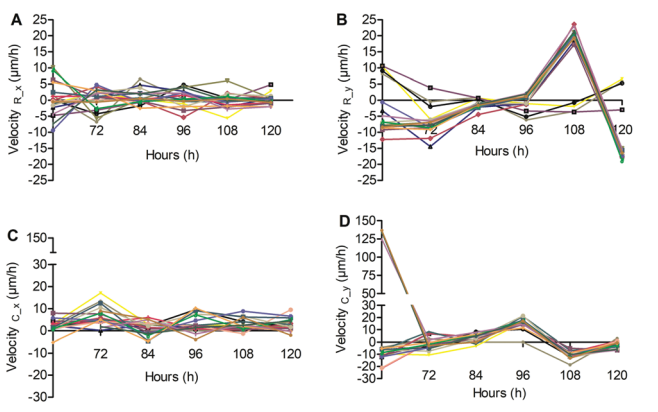


**Fig. 3** Single-cell velocity measurements. Velocities of glioma cells along the (A) $x$ and (B) $y$ axes in the regular growth medium. Velocities of glioma cells along the (C) $x$ and (D) $y$ axes in the conditional culture. Each color represents a single glioma cell.

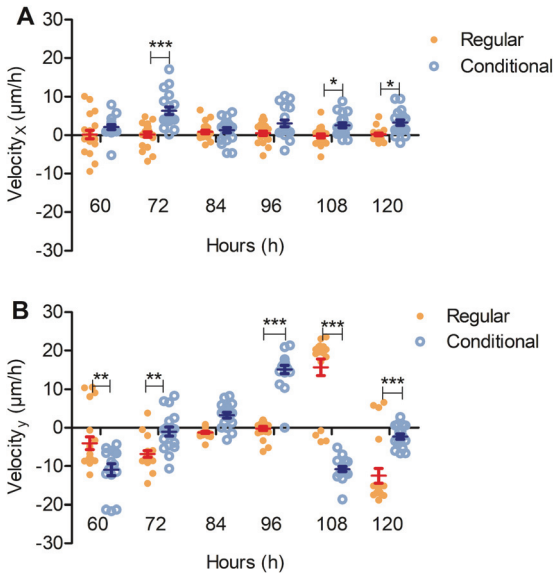


**Fig. 4** Comparison of migratory velocities of glioma cells in regular and conditional cultures. (A) $x$- and (B) $y$-axis velocities of glioma cells were compared using a two-way ANOVA comparison test. *: $p < 0.05$, **: $p < 0.01$, ***: $p < 0.001$.

the velocity distribution along the $x$ axes. There were significant differences between the velocities of glioma cells when they were cultured using regular and conditional media at 72 h ($P < 0.001$), 108 h ($p < 0.05$), and 120 h ($p < 0.05$) according to the two-way ANOVA comparison test (see the section Statistical analysis). Fig. 4B shows that glioma cells exhibited slow movement and uniform velocity distribution along the $y$ axes when they were cultured in the basal medium (Fig. 4). Conditionally cultured glioma cells exhibited significantly more differences except at 84 h (60 h and 72 h ($p < 0.01$), 96 h, 108 h, and 120 h, $p < 0.001$) in comparison with regularly cultured cells along the $y$ axes according to the two-way ANOVA comparison test (see the section Statistical analysis).

Fig. 5 shows the histogram for the migratory velocity distribution of the glioma cells presented in Fig. 3. When the cells were cultured in the regular growth medium, their mean velocities were $0.295 \pm 2.942$ μm h$^{-1}$ ($n = 120$) along the $x$ axes (Fig. 5A) and $-1.512 \pm 10.682$ ($n = 120$) along the $y$ axes (Fig. 5B). In the conditional medium, the mean velocities of glioma cells were $3.145 \pm 3.645$ ($n = 115$) along the $x$ axes (Fig. 5C) and $-0.807 \pm 9.793$ ($n = 105$) along the $y$ axes (Fig. 5D).

Fig. 6 presents the area and circularity comparisons of glioma cells when they were grown in regular and conditional media within the microchannel from 60 h to 120 h. Fig. 6A displays the change of area distributions of these two glioma cell populations at the single-cell level. The conditional growth settings increased the heterogeneity of the cellular area according to unpaired, two-tailed $t$-test results; however, the difference in the cellular area measurements between the regular and conditional cultures of glioma cells was not significant ($p =$

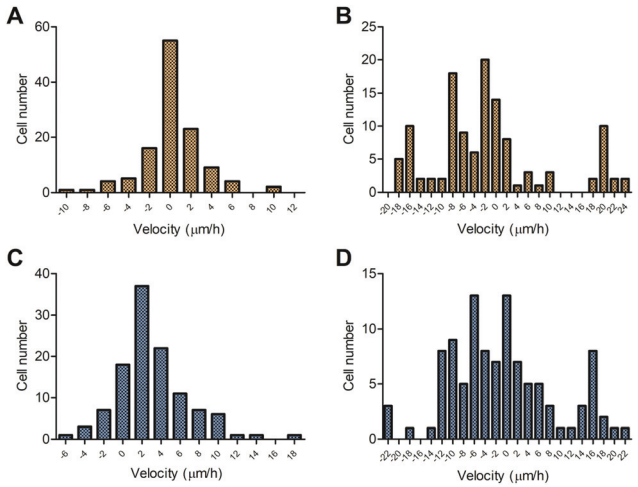


Fig. 5 Histogram of velocities for the cells displayed in Fig. 3. Velocity distribution of the glioma cells in DMEM along the *x* (A) and *y* (B) axes and in the conditional medium along the *x* (C) and *y* (D) axes.

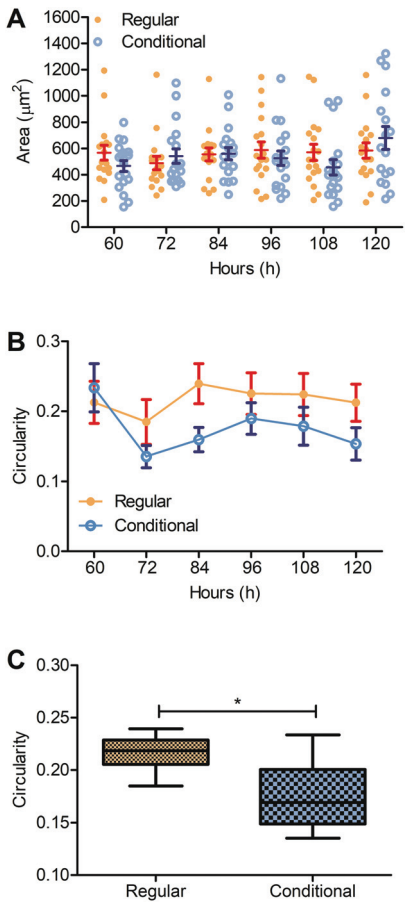


Fig. 6 Area and circularity distribution of glioma cells. (A) Area ($\mu m^2$) and (B) circularity distribution of single glioma cells in regular and conditional cultures. (C) Comparison of circularities between regular and conditional growth environments.

0.582). Fig. 6B illustrates the circularity changes of glioma cells during the 60 h regular and conditional culture. When the glioma cells were cultured in the conditional medium, they significantly lost their circularity according to the unpaired, two-tailed *t*-test ($p = 0.026$), Fig. 6C.

## Discussion

Development of new tools has prominently contributed to the understanding of aggressive glioma cell invasion at the single-cell level. Modern cell culture environments can provide precise, robust, and controllable tumor-growth conditions. Hence, the quality and quantity of data that they generate might provide new insights into the treatment of GBM or improvement of the patient prognosis. To understand the invasion behavior of glioma cells better, various techniques have been implemented, including but not limited to genomics, transcriptomics, metabolomics, proteomics, microscopy, and bioinformatics.[1–10] These tools are mostly capable of generating population-level data on glioma migration using *in vivo*, *ex vivo*, or *in vitro* growth conditions for several minutes to weeks using high-resolution imaging methods.[11–15]

Among these methodologies, *in vivo* approaches such as patient-derived xenografts in mice or rats have been more adequate to recapitulate the dynamic and highly complex nature of the GBM microenvironment. Alieva and co-workers performed *in vivo* studies *via* transplanting a GBM patient's glioma cells into a mouse brain. Their results showed that slow cells with direct movement were included in the invasive region, while the fast and randomly moving cells were in the diffusive infiltration margin of the tumor. Their results showed that the velocities of the glioma cells were 2 μm $h^{-1}$ in the core and 3–5 μm $h^{-1}$ at the margins of the tumor.[11] Farin's group transplanted the C6 glioma cells into the rats. Their findings revealed that glioma cells had an unsynchronized, saltatory migration pattern with a 25 μm $h^{-1}$ average speed. When C6 glioma cell motility was characterized by Chicoine *et al.*, they obtained 12.5 μm $h^{-1}$ and 1–3 cm $h^{-1}$ velocities *in vivo* and *in vitro*, respectively. Although these studies characterized the same cell lines using *in vivo* techniques, there are some notable variations between the results, which might reflect the heterogeneity of the glioma cells and tumor microenvironment or the reproducibility and robustness of the experimental processes. Besides, *in vivo* experiments are still very expensive, complicated, and time-consuming in comparison with *ex vivo* assays.[22–24]

*Ex vivo* experimental systems emerged to overcome the limitations of *in vivo* assays while providing a more repeatable and controllable three-dimensional (3D) microenvironment in comparison with *in vitro* assays.[24,25] Moreover, these methods can be further improved to develop precise, personalized treatment strategies using patient-derived tumor cells in their natural microenvironments.[24] Particularly, the development of human brain organoids aimed to precisely recapitulate the human brain microenvironment and overcome the limitations

of *in vivo* and *in vitro* assays.[25] Still, *in vitro* assays are among the most widely used experimental systems to investigate glioma infiltration into the brain.

Traditional two-dimensional (2D) cell culture platforms were advanced with cutting-edge microchip devices. These microfabricated tools can reflect several features of the human tumor microenvironment and still show affordability, time efficacy, observability and controllability of traditional methods while providing excellent harmony with the breakthrough imaging techniques. They can provide high-resolution, single-cell level data from a large number of cells with high sampling rates. Pioneering studies were performed using micro-patterning techniques; Kiss and his group determined the speed of U87 glioma cells of around 23 μm $h^{-1}$ (ref. 15), while Ulrich's group reported it as 35–40 μm $h^{-1}$.[16] Both investigations confirmed the heterogeneity and random movement patterns of the U87 glioma cells. In these studies, the differences between the velocity values of the glioma cells might be due to high population heterogeneity or their observation was not long enough to obtain steady-state behavior of the cells. The movement of glioma cells might exhibit directional migration or uniform velocities in longer periods. To determine the behavior of glioma cells in longer time periods, we used a microchannel shown in Fig. 1. We enumerated the mean migratory velocities of U87 glioma cells for 60 h to 120 h (Fig. 2). Our velocity measurements demonstrated that the average velocities of U87 glioma cells were around 1.5 μm $h^{-1}$ in the regular growth medium and 3.5 μm $h^{-1}$ in the conditional medium, which was composed of 50% DMEM and 50% macrophage-depleted RPMI medium, Figs. 3–5. Fig. 3 shows that the velocity changes of glioma cells were more uniform along the *x*-axis (Fig. 5A and C) than those along the *y*-axis (Fig. 5B and 5D) from 60 h to 120 h. We will further investigate the underlying reasons for the behavior of the cells that exhibited a sudden increase at 108 h along the *y* axes. Here, our aim was to present the single-cell velocity analysis of glioma cells at the steady state, starting from 60 h to 120 h, and eliminate transient migratory velocities.

Ground-breaking investigations to underline the effects of different microenvironments on glioma cell migration using microchips mostly focused on the role of ECM rigidity,[16–20,28] Recent studies presented the glioma cell motility using fibronectin-, laminin-, and collagen-coated microchannels.[16–18] The results proved that glioma cells migrated rapidly and spread extensively on highly rigid ECMs.[16,26–29] Here, we also examined the behavior of U87 glioma cells in the conditional medium that provided a molecularly rich microenvironment by macrophage-secreted molecules. It significantly affected the velocities of the glioma cells along the *x* axes, Fig. 4A ($p < 0.001$ at 72 h, $p < 0.05$ at 108 h and 120 h), and *y* axes, Fig. 4B ($p < 0.01$ at 60 h and 72 h, $p < 0.001$ at 96 h–120 h). However, the velocity distributions of the glioma cells were similar under both culture conditions, Fig. 5.

The cellular area measurements of the glioma cells in the conditional culture medium showed higher heterogeneity than those in under regular culture conditions, Fig. 6A. However, the circularity of the glioma cells was significantly reduced in the conditional culture medium ($p < 0.05$). The circularity values of the glioma cells were 0.20–0.25 in the regular medium and 0.15–0.20 in the conditional medium ($p = 0.026$), Fig. 6B and C. Recently, we showed that U87 glioma cells proliferated slightly less in the conditional medium than in the regular growth medium ($p > 0.05$).[21] Here, we report the long-term (steady state) behavior of the glioma cells using two different growth conditions in the microchip from 60 h to 120 h. We obtained consistent results with the previously published studies that demonstrated that highly motile glioma cells mostly exhibited low proliferation rates[17] with elongated morphologies[27–33] (Fig. 6). We clearly showed that macrophage-depleted medium induced a more invasive phenotype to glioma cells; they adopted spindle shapes and rapid migration velocities. Therefore, the conditional medium might contain soluble factors that affect glioma migration, infiltration, and morphology such as Chemokine C–C Ligand 5 (CCL5), Matrix Metalloproteinase 2 (MMP2), Matrix Metalloproteinase 9 (MMP9), Granulocyte-Macrophage Colony-Stimulating Factor (GM-CSF), Epidermal Growth Factor (EGF), Interleukin 1 beta (IL-1β), and Transforming Growth Factor Beta 1 (TGF-β1).[34–38] Also, we observed that the migratory velocities of glioma cells were not altered due to the geometry of circular and trapezoid pillars in the microchannel.

In the future, we plan to perform these experiments using an organotypic tumor slice culture within a microchip to determine the influence of the macrophage-depleted medium on migratory velocities of glioma cells in a brain tumor microenvironment.

## Conclusions

This study presents long-term, single-cell level migratory-velocity measurements of the U87 glioma cells under two different growth conditions using a microfluidic platform. We cultured glioma cells in the microfluidic device using either the regular growth medium or the conditional medium, which is composed of 50% basal medium and 50% macrophage-depleted medium. Here, we achieved rapid and controllable medium exchange in the microfluidic chip while acquiring better quality of cell images compared with that in a Petri dish or a well plate. Notably, we could define the exact positions of the single cells with respect to the origin, a constant reference point within the microchannel; therefore, we could precisely compare the movement of single cells with the result of several independent experiments. In previously developed microfluidic devices, migration of the glioma cells was mostly observed in the confined microchannels (2 μm × 2 μm or 3 μm × 3 μm), which limited the migration pattern and long-term observation of glioma cells.[15–20] In our microfluidic chip, glioma cells can freely move and make contact with surrounding cells, and cell growth and division can be observed for a long time. Therefore, we can obtain the population-level behavior of glioma cells at single-cell resolution. We microscopically

 

observed the behavior of the single glioma cells from 60 h to 120 h using the acquired images. We presented the mean migratory velocity values of the glioma cells as ~1.513 μm $h^{-1}$ in the basal medium and ~3.246 μm $h^{-1}$ in the conditional medium. We revealed that culturing glioma cells in the conditional medium also influenced the morphology of the glioma cells and altered their circularity. Our findings were consistent with the literature, which mostly focused on the transient behavior of the glioma cells, where the velocity measurements or the migration patterns of the glioma cells were monitored for up to 24 h. Our findings filled the gap of steady-state migratory velocity measurements of the U87 glioma cells. Also, we demonstrated that the heterogeneity of the U87 glioma cell population increased when their culture medium was supplemented with the macrophage-depleted medium. We plan to perform these measurements using an organotypic tumor slice culture within a microchip to introduce the complex nature of the tumor microenvironment into our quantifications.

## Author contributions

Conceptualization, M.E.; methodology, M.E. and E.S.; validation, M.E. and E.S; formal analysis, E.S.; investigation, M.E. and E.S.; resources, M.E.; writing—original draft preparation, E.S.; writing—review and editing, M.E.; visualization, M.E. and E.S.; supervision, M.E.; project administration, M.E., funding acquisition, M.E. All authors have read and agreed to the published version of the manuscript.

## Conflicts of interest

There are no conflicts to declare.

## Acknowledgements

This research was partially funded by he Scientific and Technological Research Council of Turkey (TUBITAK), grant number “217S616”.

## References

1 E. Jung, *et al.*, *Nat. Commun.*, 2021, **12**, 1014.
2 M. der, M. Inda, R. Bonavia and J. Seoane, *Cancers*, 2014, **6**, 226–239.
3 E. C. Holland, *Proc. Natl. Acad. Sci. U. S. A.*, 2000, **97**, 6242–6244.
4 A. Vollmann-Zwerenz, *et al.*, *Int. J. Mol. Sci.*, 2020, **21**, 1932.
5 F. Lefrance, *Cancer Treat. Rev.*, 2018, **68**, 145–154.
6 A. Claes, A. J. Idema and P. Wesseling, *Acta Neuropathol.*, 2007, **114**, 443–458.
7 K. Jiang, *et al.*, *Cell Death Dis.*, 2020, **11**, 88.
8 L. Soroceanu, T. J. Manning, Jr. and H. Sontheimer, *J. Neurosci.*, 1999, **19**, 5942–5954.
9 K. Aldape, *et al.*, *Acta Neuropathol.*, 2015, **129**, 829–848.
10 C. L. Gladson, R. A. Prayson and W. M. Liu, *Annu. Rev. Pathol.*, 2010, **5**, 33–50.
11 M. Alieva, *et al.*, *Sci. Rep.*, 2014, **9**, 2054.
12 T. Demuth, *et al.*, *Clin. Exp. Metastasis*, 2001, **18**, 589–597.
13 M. R. Chicoine and D. L. Silbergeld, *J. Neurosurg.*, 1995, **82**, 615–622.
14 A. Farin, *et al.*, *Glia*, 2006, **53**, 799–808.
15 A. Kiss, *et al.*, *PLoS One*, 2014, **9**, e93431.
16 T. A. Ulrich, E. M. de Juan Pardo and S. Kumar, *Cancer Res.*, 2009, **69**, 4167–4174.
17 A. Fayzullin, *et al.*, *Transl. Oncol.*, 2019, **12**, 122–133.
18 P. Monzo, *et al.*, *Mol. Biol. Cell*, 2016, **27**, 1246–1261.
19 L. S. Prahl, *et al.*, *bioRxiv*, 2018, 500843.
20 S. Sheykhzadeh, *et al.*, *Sci. Rep.*, 2020, **10**, 2320.
21 E. Sengul and M. Elitas, *Micromachines*, 2020, **11**, 845.
22 P. Gritsenko, W. Leenders and P. Friedl, *Hostochem. Cell Biol.*, 2017, **148**, 359–406.
23 T. Eisemann, *et al.*, *BMC Cancer*, 2018, **18**, 103.
24 G. Goranci-Buzhala, *et al.*, *Cell Rep.*, 2020, **31**, 107738.
25 K. Aldape, *et al.*, *Nat. Rev. Clin. Oncol.*, 2019, **16**, 509–520.
26 A. Linkous, *et al.*, *Cell Rep.*, 2019, **26**, 3203–3211.
27 I. Koh, J. Cha, J. Park, J. Choi, S.-G. Kang and P. Kim, *Sci. Rep.*, 2018, **8**, 4608.
28 C. M. Lo, H. B. Wang, M. Dembo and Y. L. Wang, *Biophys. J.*, 2000, **79**, 144–152.
29 A. Rape, B. Ananthanarayanan and S. Kumar, *Adv. Drug Delivery Rev.*, 2014, **79–80**, 172–183.
30 H. Hatzikirou, *et al.*, *Math. Med. Biol.: J. IMA*, 2012, **29**, 49–65.
31 P. Friedl and S. Alexander, *Cell*, 2011, **147**, 992–1009.
32 B. L. Bangasser, *et al.*, *Nat. Commun.*, 2017, **8**, 15313.
33 J. J. Parker, *et al.*, *Sci. Rep.*, 2018, **8**, 18002.
34 C. Y.-J. Wu, *et al.*, *Neuro. Oncol.*, 2020, **22**, 253–266.
35 M. Osswald, *et al.*, *Nature*, 2015, **528**, 93–98.
36 Y. Peng, *et al.*, *Brain Sci. Adv.*, 2021, **6**, 306–323.
37 M. Gjorgjevski, *et al.*, *Biosci. Rep.*, 2019, **39**, BSR20182361.
38 A. Wesolowska, *et al.*, *Oncogene*, 2007, **27**, 918–930.